

## Alignment and orientation of absorbed dipole molecules

Y. Y. Liao, Y. N. Chen, and D. S. Chuu\*

*Department of Electrophysics, National Chiao-Tung University, Hsinchu 300, Taiwan*

(Received 18 April 2004; revised manuscript received 27 July 2004; published 29 December 2004)

Half-cycle laser pulse is applied on an absorbed molecule to investigate its alignment and orientation behavior. Crossover from field-free to hindered rotation motion is observed by varying the angle of hindrance of potential well. At small hindered angle, both alignment and orientation show sinusoidal-like behavior because of the suppression of higher excited states. However, mean orientation decreases monotonically as the hindered angle is increased, while mean alignment displays a minimum point at certain hindered angle. The reason is attributed to the symmetry of wave function and can be explained well by analyzing the coefficients of eigenstates.

DOI: 10.1103/PhysRevB.70.233410

PACS number(s): 73.20.Hb, 33.55.Be, 33.20.Sn

Alignment and orientation of molecules are important in the investigations of stereodynamics,<sup>1</sup> surface catalysis,<sup>2</sup> molecular focusing,<sup>3</sup> and nanoscale design.<sup>4</sup> The alignment scheme has been demonstrated both in adiabatic and non-adiabatic regimes. A strong laser pulse can adiabatically create pendular states, and the molecular axis is aligned in parallel to the direction of field polarization. The molecule goes back to its initial condition after the laser pulse is switched off, and the alignment can no longer be observed again.<sup>5</sup> To achieve adiabatic alignment, the duration of laser pulse must be longer than the rotational period. However, an ultrashort laser pulse with several cycles is also observed to induce a field-free alignment providing the duration of laser pulse is smaller than the rotational period. In this limit, the alignment occurs periodically in time as long as the coherence of the process is preserved.<sup>6</sup> On the other hand, a femtosecond laser pulse is found to be able to generate field-free orientations.<sup>7</sup> The dipole molecule, kicked by an impulsive pulse, will tend to orient in the direction of laser polarization. Laser-induced molecular orientations have been demonstrated in several experiments.<sup>8-10</sup>

Recently, the rotational motion of a molecule interacting with a solid surface has attracted increasing interest. It is known that molecules can be desorbed by applying UV laser beam along the surface direction, and the quadrupole is a measure of the rotational alignment.<sup>11</sup> To understand molecular-surface interaction, Gadzuk and his co-workers<sup>12</sup> proposed an infinite-conical-well model, in which the adsorbed molecule is only allowed to rotate within the well region. Shih *et al.* further proposed a finite-conical-well model to generalize the study of a finite hindrance.<sup>13</sup> Their results showed that the rotational states of an adsorbed dipole molecule in an external electric field exhibit interesting behaviors, and theoretical calculation of the quadrupole moment based on finite-conical-well model is in agreement with the experimental data.<sup>14</sup> These findings may be very useful for understanding the surface reaction.

In the present work we present a detailed investigation on the rotational motion of a polar diatomic molecule, which is confined by a hindering conical well. Different well-dependent signatures between the alignment and orientation of the hindered molecule under an ultrashort laser pulse are pointed out for the first time. Crossover from field-free to

hindered rotation is also observed by varying the hindered angle of potential well. These make our results promising and may be useful in understanding the molecule-surface interactions.

Consider now a laser pulse polarizing in the  $z$  direction interacts with the hindered molecule as shown in Fig. 1. The model Hamiltonian can be written as

$$H = \frac{\hbar^2}{2I} J^2 + V_{hin}(\theta, \phi) + H_I, \quad (1)$$

where  $J^2$  and  $I$  are angular momentum and moment of inertia of the molecule. The rotational constant  $B$  is set equal to  $\hbar^2/2I$ . It is reasonable to assume that the surface potential  $V_{hin}(\theta, \phi)$  is independent of  $\phi$  since previous calculations have shown that its dependence on  $\phi$  is weaker than that on  $\theta$ .<sup>15-17</sup> Therefore, in the vertical absorbed configuration, the surface potential can be written as<sup>12</sup>

$$V_{hin}(\theta) = \begin{cases} 0, & 0 \leq \theta \leq \alpha \\ \infty, & \alpha < \theta \leq \pi, \end{cases} \quad (2)$$

where  $\alpha$  is the hindered angle of the conical well. In Eq. (1),  $H_I$  describes the interaction between the dipole moments (permanent and induced) and laser field:

$$H_I = -\mu E(t) \cos \theta - \frac{1}{2} E^2(t) [(\alpha_{\parallel} - \alpha_{\perp}) \cos^2 \theta + \alpha_{\perp}], \quad (3)$$

where  $\mu$  is the dipole moment. The components of the polarizability  $\alpha_{\parallel}$  and  $\alpha_{\perp}$  are parallel and perpendicular to the

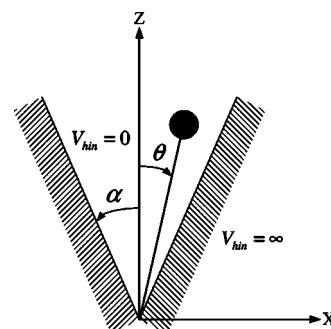


FIG. 1. Schematic view of the hindered rotor.

molecular axis, respectively. The laser field in our consideration is a Gaussian shape:  $E(t) = Ee^{-(t-t_0)^2/\sigma^2} \cos(\omega t)$ , where  $E$  is the field strength and  $\omega$  is the laser frequency. To solve the time-dependent Schrödinger equation, the wave function is expressed in terms of a series of eigenfunctions as

$$\Psi_{l,m} = \sum c_{l,m}(t) \psi_{l,m}(\theta, \phi), \quad (4)$$

where  $c_{l,m}(t)$  are time-dependent coefficients corresponding to the quantum numbers  $(l,m)$ . For the vertical adsorbed configuration, the wave function can be written as

$$\psi_{l,m}(\theta, \phi) = \begin{cases} A_{l,m} P_{\nu_{l,m}}^{|m|}(\cos \theta) \frac{\exp(im\phi)}{\sqrt{2\pi}}, & 0 \leq \theta \leq \alpha \\ 0, & \alpha < \theta \leq \pi, \end{cases} \quad (5)$$

where  $A_{l,m}$  is the normalization constant and  $P_{\nu_{l,m}}^{|m|}$  is the associated Legendre function of arbitrary order. In the above equations, the molecular rotational energy can be expressed as

$$\epsilon_{l,m} = \nu_{l,m}(\nu_{l,m} + 1)B. \quad (6)$$

In order to determine  $\nu_{l,m}$ , one has to match the boundary condition

$$P_{\nu_{l,m}}^{|m|}(\cos \alpha) = 0. \quad (7)$$

After determining the coefficients  $c_{l,m}(t)$ , the orientation  $\langle \cos \theta \rangle$  and alignment  $\langle \cos^2 \theta \rangle$  can be carried out immediately.

We choose ICI as our model molecule, with dipole moment  $\mu = 1.24$  Debye, rotational constant  $B = 0.114 \text{ cm}^{-1}$ , polarizability components  $\alpha_{\parallel} \approx 18 \text{ \AA}^3$  and  $\alpha_{\perp} \approx 9 \text{ \AA}^3$ . The peak intensity and frequency of laser pulse are about  $5 \times 10^{11} \text{ W/cm}^2$  and  $210 \text{ cm}^{-1}$ , respectively. For simplicity (zero-temperature case), the rotor is assumed in ground state initially, i.e.,  $c_{0,0}(t=0) = 1$ . Besides, in order to keep the simulations promising, the highest quantum number for numerical calculations is  $l = 15$ , such that the results are convergent and the precision is to the order of  $10^{-7}$ .

The solid lines in the insets of Fig. 2 show the dependence of the alignment on hindered angle  $\alpha$ . For  $\alpha = 60^\circ$ , sinusoidal-like behavior is presented, and the alignment ranges from 0.63 to 0.91. As the hindered angle increases, the curves become more and more complicated and gradually approach the free rotor limit as shown in the insets of Fig. 2(b) ( $\alpha = 120^\circ$ ) and 2(c) ( $\alpha = 180^\circ$ ). This can be understood well by studying the populations  $|c_{l,m}|^2$  of low-lying states. In the regime of the small hindered angle, there is little chance for electrons to populate in higher excited states since the shrinking of the conical-well angle causes the increasing of energy spacings.

One also notes that the populations of a hindered molecule for  $\alpha = 60^\circ$  and  $120^\circ$ , shown in Figs. 2(a) and 2(b), are mainly composed of  $l=0, 1$  and  $2$  states, while the population of a free rotor is composed of  $l=0, 2$ , and  $4$  states. The underlying physics comes from the reason that  $\langle \psi_{l',m'} | \cos^2 \theta | \psi_{l,m} \rangle$  is nonzero for all  $l$  and  $l'$  values in the

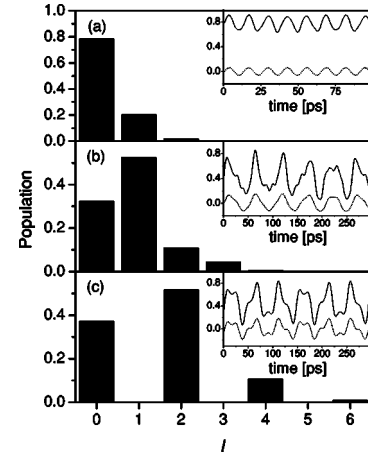


FIG. 2. The populations of the states  $(l, m=0)$  for different hindered angles: (a)  $\alpha = 60^\circ$ , (b)  $\alpha = 120^\circ$ , (c)  $\alpha = 180^\circ$ . The insets show the corresponding alignments (solid lines) and the first two main contributions of the factors  $\sum_{l' \neq l} \langle \psi_{l',m'} | \cos^2 \theta | \psi_{l,m} \rangle$  (dotted lines).

case of hindered rotation. But it is zero in free rotor limit except for  $l=l'$  or  $l=l' \pm 2$ . The dotted lines in the insets represent the first two main contributions of the factors  $\sum_{l' \neq l} \langle \psi_{l',m'} | \cos^2 \theta | \psi_{l,m} \rangle$  summed from low-lying states, i.e., the sum of the largest two values of the off-diagonal term  $\langle \psi_{l',m'} | \cos^2 \theta | \psi_{l,m} \rangle$ . As can be seen, the populations for the small hindered angle are mainly distributed on lower states since the main oscillation feature (e.g., the frequency) of the curve (dotted lines) is quite similar to that from whole contributions (solid lines).

Let us now turn our attention to the case of orientation. After applying a short pulse laser, the orientation  $\langle \cos \theta \rangle$  of a hindered molecule ( $\alpha = 60^\circ$ ) oscillates sinusoidally with time as shown in Fig. 3(a). The value of  $\langle \cos \theta \rangle$  is always positive because the rotational wave function is compressed heavily. As the hindered angle  $\alpha$  becomes larger, the oscillation fre-

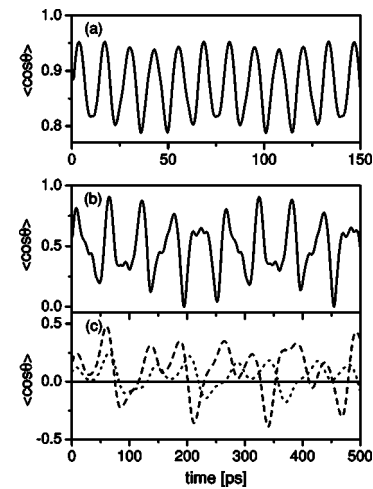


FIG. 3. The orientations  $\langle \cos \theta \rangle$  (solid lines) of a hindered molecule confined by an infinite conical-well for different hindered angles: (a)  $\alpha = 60^\circ$ , (b)  $\alpha = 120^\circ$ , and (c)  $\alpha = 175^\circ$ . The dashed and dotted lines in (c) correspond to different potential barrier height, i.e.,  $V_0 = \infty$  and  $100$ , respectively.

quency also decreases as shown in Fig. 3(b). These signatures are quite close to that of the alignment. We then conclude that even at larger hindered angle ( $\alpha=120^\circ$ ) the role of hindered potential still overwhelms the laser pulse, otherwise, the value of  $\langle \cos \theta \rangle$  should not always be positive.

Figure 3(c) represents results of orientations in infinite ( $V_0=\infty$ ) or finite ( $V_0=100$ ) conical-well potential for  $\alpha=175^\circ$ . Dashed and dotted lines correspond to  $V_0=\infty$  and 100, respectively. For the case of finite conical-well potential, the wave function is expressed in terms of a series of the basis wave functions obtained in Refs. 13 and 14. As can be seen, the effect of the laser pulse is obvious because a negative value appears. Comparing the results with the free orientation,<sup>7</sup> the angular distributions for the finite well are more isotropic since the wave functions can penetrate into the conical barrier.

Further analysis shows that components of orientation  $\langle \cos \theta \rangle$  or alignment  $\langle \cos^2 \theta \rangle$  can be divided into two parts: diagonal and nondiagonal terms. The nondiagonal term represents the variations of these curves such as those in the insets of Fig. 2. These variations with time are determined by the phase difference coming from various energy levels. To see the contributions from diagonal terms, we evaluate the time-averaged orientation and alignment. In this case, the nondiagonal values will be averaged out, and only contributions from diagonal terms exit. Figure 4 shows the mean orientation and alignment as a function of hindered angle. As  $\alpha$  increases, the mean orientation decreases monotonically from 1 to 0. This is because the mean orientation is determined by  $|c_{l,m}|^2$  and  $\langle \psi_{l,m} | \cos \theta | \psi_{l,m} \rangle$ . For a larger angle  $\alpha$ , the populations  $|c_{l,m}|^2$  is mainly composed of  $l=0, 2, 4$  states. But the value  $\langle \psi_{l,m} | \cos \theta | \psi_{l,m} \rangle$  is governed by the selection rule:  $l=l'+1$ . Thus the net effect is the shrinking of the mean orientation in the large angle limit.

Contrary to orientation, the mean alignment shows a quite different feature. The value of  $\langle \cos^2 \theta \rangle$  first decreases as  $\alpha$  increases. However, it reaches a minimum point about  $\alpha=140^\circ$ . From the insets of Fig. 4, we know that the values of  $(\langle \psi_{l,m} | \cos^2 \theta | \psi_{l,m} \rangle)$  do not depend significantly on  $\alpha$ . Therefore, the decrease of  $\langle \cos^2 \theta \rangle$  comes from the decreasing tendency of the population  $|c_{l=1,m}|^2$ , while its increasing behavior is caused by two other populations  $|c_{l=0,m}|^2$  and  $|c_{l=2,m}|^2$ . Competition between these two effects results in a minimum point.

A few remarks about experimental verifications should be mentioned here. The degree of alignment can be measured

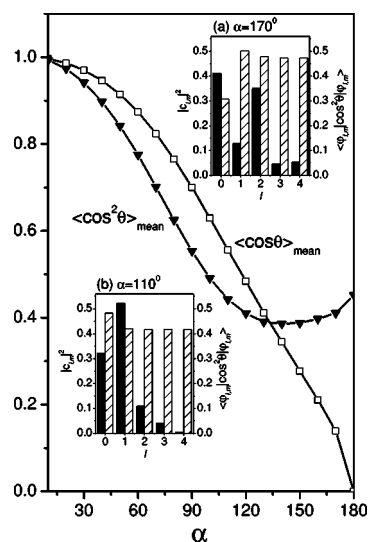


FIG. 4. The mean orientation  $\langle \cos \theta \rangle_{\text{mean}}$  and alignment  $\langle \cos^2 \theta \rangle_{\text{mean}}$  in an infinite conical well. The insets show the populations  $|c_{l,m}|^2$  (solid bar) and factors  $\langle \psi_{l,m} | \cos^2 \theta | \psi_{l,m} \rangle$  (striped bar). Insets (a) and (b) correspond to  $\alpha=110^\circ$  and  $\alpha=170^\circ$ , respectively.

with the techniques of the femtosecond photodissociation spectroscopy and the ion imaging.<sup>8</sup> The alignment is probed by breaking the molecular bond and subsequently measuring the direction of the photofragments by a mass selective position sensitive ion detector. In contrast to alignment, the orientation is probed by Coulomb exploding the molecules with a femtosecond laser pulse.<sup>9</sup> By detecting the fragment ions with the time-of-flight mass spectrometer, a significant asymmetry should be observed in the signal magnitudes of the forward and the backward fragments. Under proper arrangements, orientation and alignment of an absorbed molecule may be examined by these spectroscopic technologies.

In conclusion, we have shown that a short laser pulse can induce alignment and orientation of a hindered molecule. The hindered angle of the hindered potential well plays a key role on the molecular alignment and orientation. Crossover from field-free rotation to a hindered one can be observed by varying the hindered angle of the potential well. Time-averaged alignment and orientation are investigated thoroughly to understand the difference between these two quantities.

This work is supported partially by the National Science Council, Taiwan under Grant No. NSC 92-2120-M-009-010.

\*Corresponding author. Email address: dschuu@mail.nctu.edu.tw

<sup>1</sup>Special issue on Stereodynamics of Chemical Reaction [J. Phys. Chem. A **101**, 7461 (1997)].

<sup>2</sup>V. A. Cho and R. B. Bernstein, J. Phys. Chem. **95**, 8129 (1991).

<sup>3</sup>H. Stapelfeldt, H. Sakai, E. Constant, and P. B. Corkum, Phys. Rev. Lett. **79**, 2787 (1997).

<sup>4</sup>T. Seideman, Phys. Rev. A **56**, R17 (1997); R. J. Gordon, L. Zhu, W. A. Schroeder, and T. Seideman, J. Appl. Phys. **94**, 669

(2003).

<sup>5</sup>B. Friedrich and D. Herschbach, Phys. Rev. Lett. **74**, 4623 (1995); L. Cai, J. Marango, and B. Friedrich, Phys. Rev. Lett. **86**, 775 (2001).

<sup>6</sup>J. Ortigoso, M. Rodriguez, M. Gupta, and B. Friedrich, J. Chem. Phys. **110**, 3870 (1999); M. Machholm, *ibid.* **115**, 10724 (2001).

<sup>7</sup>M. Machholm and N. E. Henriksen, Phys. Rev. Lett. **87**, 193001

- (2001).
- <sup>8</sup>W. Kim and P. M. Felker, *J. Chem. Phys.* **104**, 1147 (1996); **108**, 6763 (1998); H. Sakai *et al.*, *ibid.* **110**, 10235 (1999); J. J. Larsen *et al.*, *ibid.* **111**, 7774 (1999).
- <sup>9</sup>H. Sakai, S. Minemoto, H. Nanjo, H. Tanji, and T. Suzuki, *Phys. Rev. Lett.* **90**, 083001 (2003); S. Minemoto, H. Nanjo, H. Tanji, T. Suzuki, and H. Sakai, *J. Chem. Phys.* **118**, 4052 (2003).
- <sup>10</sup>V. Renard, M. Renard, S. Guérin, Y. T. Pashayan, B. Lavorel, O. Faucher, and H. R. Jauslin, *Phys. Rev. Lett.* **90**, 153601 (2003).
- <sup>11</sup>I. Beauport, K. Al-Shamery, and H.-J. Freund, *Chem. Phys. Lett.* **256**, 641 (1996); S. Thiel, M. Pykavy, T. Klüner, H.-J. Freund, R. Kosloff, and V. Staemmler, *Phys. Rev. Lett.* **87**, 077601 (2001); *J. Chem. Phys.* **116**, 762 (2002).
- <sup>12</sup>J. W. Gadzuk, U. Landman, E. J. Kuster, C. L. Cleveland, and R. N. Barnett, *Phys. Rev. Lett.* **49**, 426 (1982).
- <sup>13</sup>Y. T. Shih, D. S. Chuu, and W. N. Mei, *Phys. Rev. B* **51**, 14 626 (1995); **54**, 10 938 (1996).
- <sup>14</sup>Y. T. Shih, Y. Y. Liao, and D. S. Chuu, *Phys. Rev. B* **68**, 075402 (2003).
- <sup>15</sup>R. P. Pan, R. D. Eters, K. Kobashi, and V. Chandrasekharan, *J. Chem. Phys.* **77**, 1035 (1982).
- <sup>16</sup>J. W. Riehl and C. J. Fisher, *J. Chem. Phys.* **59**, 4336 (1973).
- <sup>17</sup>V. M. Allen and P. D. Pacey, *Surf. Sci.* **177**, 36 (1986).